

# **Seismic Structure-Soil-Structure Interaction (SSSI) between piled neighboring bridges: Influence of height ratio**

*Mohanad Talal Alfach*

*School of Mathematics, Computer Science and Engineering, Department of Civil Engineering*

*City, University of London, UK*

*Email: [mohanad.alfach@yahoo.com](mailto:mohanad.alfach@yahoo.com)*

## **Abstract**

This paper investigates the influence of the height ratios of three dissimilar adjacent bridges with different superstructure masses [ $M_{st}=350, 1050, 350$  Tons] on the seismic Structure-Soil-Structure Interaction (SSSI) through 3D numerical simulations. To this end, an extensive series of numerical analyses have been performed for a range of height ratios (R) (R=1,1.1,1.15, 1.2, 1.25, 1.5, 2, and 3) focusing on its impacts on the superstructure acceleration and the internal forces induced in the foundations' piles. The considered bridges are founded on groups of piles implanted in nonlinear clay. The numerical analyses have been carried out using a Three-dimensional finite differences modeling software FLAC 3D (Fast Lagrangian analysis of continua in 3 dimensions). The results show that the mass ratios change significantly the (SSSI) effects on the superstructure acceleration and the piles internal forces. Importantly it is demonstrated that the adverse effects of mass ratios are more pronounced for the height ratios of (R= 1.1, and 1.2) which incite increase in the bending moment, shear force and the superstructure acceleration by (up to 237.8 %, 291.4 %, and 70.33% respectively). Contrarily, the bending moment, shear force and the superstructure acceleration decrease by (up to 72 %, 82.14 %, and 81.13 % respectively) for mass ratio of (R= 3). This suggests that careful arrangement of adjacent structures with different masses could be used efficiently to control the (SSSI) effects.

## **Keywords**

SSSI, different superstructure masses, height ratios, dissimilar adjacent bridges, nonlinear, seismic, three-dimensional.

## 1 Introduction

The increasing shortage of land resources in the urban areas due to the huge population growth has become a major issue to consider with the rapid urbanization in large cities. As structures clusters got denser and denser, the dynamic interaction of adjacent structures in cities and urban areas through the soil medium is inevitable. This effect is termed Structure-Soil-Structure Interaction (SSSI). For the sustainable development of these crowded cities, it is more and more necessary to study the effects of (SSSI) in order to ensure a good earthquake resilience of dense urban buildings. The majority of the recent (SSSI) studies have focused on the inevitable seismic interaction between the neighboring structures, particularly the tall buildings and the skyscrapers. Very few research have addressed the seismic interaction between adjacent bridges, which their seismic behavior poses a special challenge, as they have unique features like their long structures supported on multiple piers with varying foundation types and subsurface conditions. Therefore, this study focuses on the seismic interaction between dissimilar neighboring bridges in Highways and Roads intersections (in different directions and levels) with different superstructure masses ratios, and the effects of the clear distances between the adjacent bridges are extensively examined to assess their importance.

The significance of studying the constructive/destructive or neutral structural effects of the (SSSI) between clusters of adjacent structures has received sustained attention in last decades. Alexander et al. [4] proposed a discrete rotational spring element for connecting adjacent foundations, however, the vertical and horizontal degree-of-freedom connectivity is not discussed. The rotational spring element was calibrated using data from both static and dynamic finite elements models. Also, Alam and Kim [2] conducted a comprehensive numerical study focusing on the effects of spatial variation of earthquake ground motion on the responses of adjacent reinforced concrete (RC) frame structures. Ghiocel et al. [10] investigated the (SSSI) effects in densely built urban areas for a 15 floor Multistorey Building (MB), a Church Building (CB), and a Subway Station (SS) in the Bucharest city. They denoted that the responses of adjacent structures have changed remarkably due to spatial variation of ground motions. Likewise, three-dimensional finite element models of tall buildings on different flexible foundation soils have been used by Rahgozar [12] to assess the effects of (SSSI) between the neighboring 15 and 30 story steel structures founded on sandy and clayey soils. Ghandil and Aldaikh [9] conducted a series of models considering (SSSI) focusing on pounding problem of two adjacent symmetric in plan buildings excited by seismic loadings They confirmed that at least three times, the International Building Code 2009 minimum inter-building spacing advised value is required as a clear distance for adjacent symmetric buildings to prevent the occurrence of seismic pounding. A two-dimensional simple discrete nonlinear model has been used by Vicencio and Alexander [13] to evaluate the effect of (SSSI) between two buildings given different parameters of the buildings, inter-building spacing, and soil type. Wang [15] carried out a numerical study on the dynamic interaction between underground station and nearby surface structure founded on viscous-elastic soil layer, under vertically incident S wave. While Alfach [3] has studied the (SSSI) effects between two dissimilar bridges supported by piles implanted in nonlinear clay. A detailed series of numerical analyses have been employed to investigate the effect of inter-bridge spacing and the plan positioning of the bridges towards the seismic loading direction. Likewise, Liang et al. [11] employed a 2D numerical model to investigate (SSSI) interaction for two similar structures supported by stiff foundations implanted in a layered half-space. Also, Ada et al. [1] have numerically analyzed the effects of (SSSI) on the seismic behavior of adjacent frame structures. They have investigated the impacts of the distances between the structures, number of stories, soil rigidity, seismic loading, and scheme of the structures. In a similar manner, Bybordiani and Arici [7] have employed detailed finite element models of 5-, 15-, and 30-story clusters structures founded on the viscoelastic half-space to rigorously investigate the interacting effects of adjacent

buildings in a two-dimensional. The effects of the foundation material and the distance between adjacent buildings on the structural behavior of the neighboring buildings were discussed. They asserted the negligible effects of (SSSI) between identical low-rise structures. conversely, the (SSSI) between high-rise structures induced a considerable increase in the true seismic demands. Vicencio et al. [14] assessed the effects of (SSSI) between two adjacent buildings, one of which was dissymmetrical in plan. The results illustrated that the (SSSI) can considerably affect the acceleration and displacement response of the asymmetrical plan structures. Similarly, Gan et al. [8] conducted a comprehensive numerical study of (SSSI) between three neighboring structures with pile-raft foundations under seismic loading. The results showed that the (SSSI) could have positive or negative effects on the structural seismic response of the structures. Similarly, Bolisetti and Whittaker [6] explored the (SSSI) effects between low-rise to medium-rise buildings by comparing their numerical simulation analyses with data from a set of centrifuge experiments of similar models.

### ***1.1 Aims***

In this paper, we extend our previous study Alfach [3] on the (SSSI) of two dissimilar bridges with different superstructure mass ratios, to the case of three dissimilar bridges with different superstructure height and mass ratios. The three dissimilar bridges are supported by piles embedded in nonlinear clay. while the concrete behavior is simulated by using a linear model. The numerical analyses were carried out by using a three-dimensional finite-difference modeling code (FLAC 3D).

We will focus in this study on the effect of the inter-bridge spacing. The aim of this paper is to answer the following questions.

- Do the (SSSI) effects between three dissimilar bridges with different superstructure height and mass ratios are adverse, beneficial, or neutral to a level at which it can be safely neglected?
- Does decreasing inter-bridge spacing would amplifier (SSSI) effects?

## **2 Numerical model of adjacent bridges**

### ***2.1 Soil-pile-bridge model***

Two 3-dimensional (3D) bridges with different deck lumped masses (350, and 1050 Tons) are studied here for developing various neighborhood combinations. The bridges are supported by groups of floating reinforced-concrete piles (6, and 18 piles) respectively, in order to keep the static load supported by each pile is equal to 80 tons. The piles with a length of ( $L_p = 10.5$  m) and a diameter of ( $D_p = 0.8$  m) are rigidly connected in the reinforced concrete cap of (1 m) thick as shown in figure (1). These piles are embedded into a homogeneous nonlinear cohesive soil layer ( $C=150$  KPa,  $\varphi = 0$ ) underlined by rigid bedrock (Figure 2). An elastoplastic law without hardening based on the standard Mohr-Coulomb criterion is used for modeling the soil material behavior. The fundamental geotechnical properties of the soil layer are summarized in table (1). The comportment of the structural elements in the model: the piles-cap, bridge pier, and the deck (superstructure) mass are supposed to be elastic. The characteristics of the superstructure and the pile groups are summarized in tables (2) and (3) respectively.

**Table 1.** Properties of cohesive soil.

$\rho_s$ (kg/m <sup>3</sup> )	$E_{os}$ (MPa)	$v_s$	$K_o$	$\zeta_s$ (%)	$C$ (kPa)	$\varphi$ (°)	$\Psi$ (°)
1700	8	0.3	0.5	5	150	0	0

**Table 2.** Elastic characteristics of the Superstructure

$\rho_{st}$ (kg/m <sup>3</sup> )	$E_{st}$ (MPa)	$v_{st}$	$\xi_{st}$ (%)	Masse (Tons)
2500	8000	0.3	2	350

Where  $\rho_{st}$ ,  $E_{st}$  and  $v_{st}$  are the density, young's modulus and the coefficient of Poisson's ratio.  $\xi_{st}$ : is the percentage of critical damping.  $D_p$ : is the pile diameter.  $E \cdot A$  and  $E \cdot I$  are the axial and bending stiffness.

**Table 3.** Elastic characteristics of the Piles materials

Material	Diameter (m)	Mass Density $\rho$ (kg/m <sup>3</sup> )	Young Modulus $E$ (MPa)	Poisson ratio $\nu$	Damping ratio $\xi$ (%)	Height (m)
Pile	0.8	2500	20000	0.3	2	10

Considering the high sensitivity of the problem of seismic-structure interaction (SSSI), a few arrangements were taken:

- The inter-piles spacing was adopted as ( $S = 3.75 \cdot D_p = 3$  m) in order to prevent the potential pile-pile interaction.
- The cap was placed a 0.5 m above the soil surface with the purpose of deterring the possible soil-cap interaction.
- In order to minimize the influence of seismic wave's reflection on the structural model, the absorbent boundaries have been employed.
- Aiming to minimize the numerical analysis cost, the soil model has meshed with increasing density away from the top-center of the soil domain where we presume significant structure-soil-structure effects as shown in figure (2).

In order to enhance the numerical stability of the analyses, slight damping of Rayleigh-type is used for the soil and the structure. A 0.02 damping ratio is used for the structural elements and 0.05 for the soil, Chopra. [5]. The superstructure is modeled by decks lumped masses [ $M_{st}=350$ , and 1050 Tons] respectively, supported by pillars. The flexural modal rigidity of the superstructure is [ $K_{st} = 86840, 1389440, 1389440$  KN/m] respectively, and its frequencies (assumed fixed at the base) are equal to [ $F_{st}=2.5$ , and 5.78 Hz] respectively. Those values were calculated by the following formulations:

$$f_{st} = \frac{1}{2\pi} \sqrt{\frac{K_{st}}{M_{st}}} , \quad K_{st} = \frac{3EI_{st}}{H_{st}^3} \quad (1)$$

While the fundamental frequency of the soil layer is 3.2 Hz. The flexible base frequencies of the superstructure taking into consideration the soil-structure interaction were calculated (using numerical methods) as  $F_{st,flex}=0.827$ , and 0.7 Hz respectively.

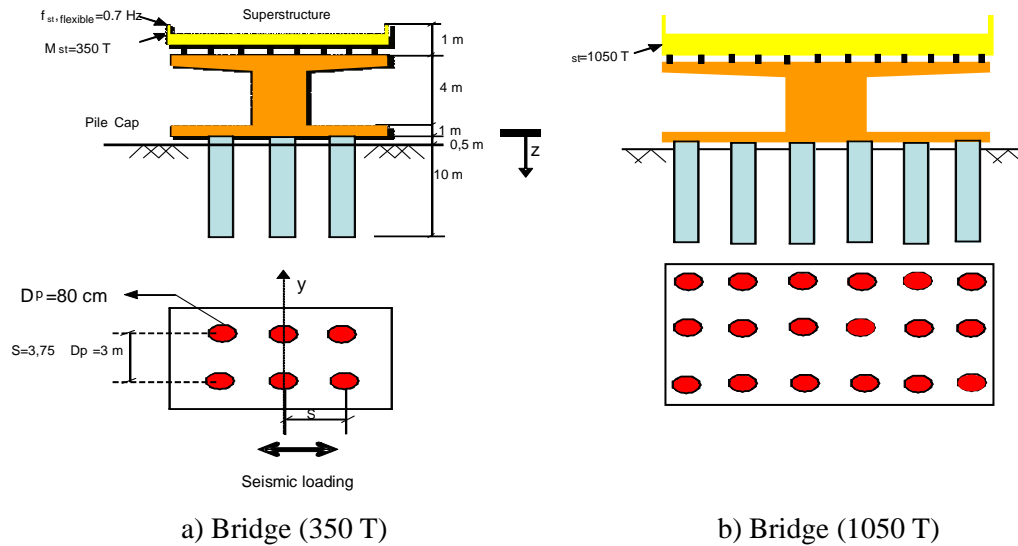


**Fig. 1** Piles-Bridge system geometry

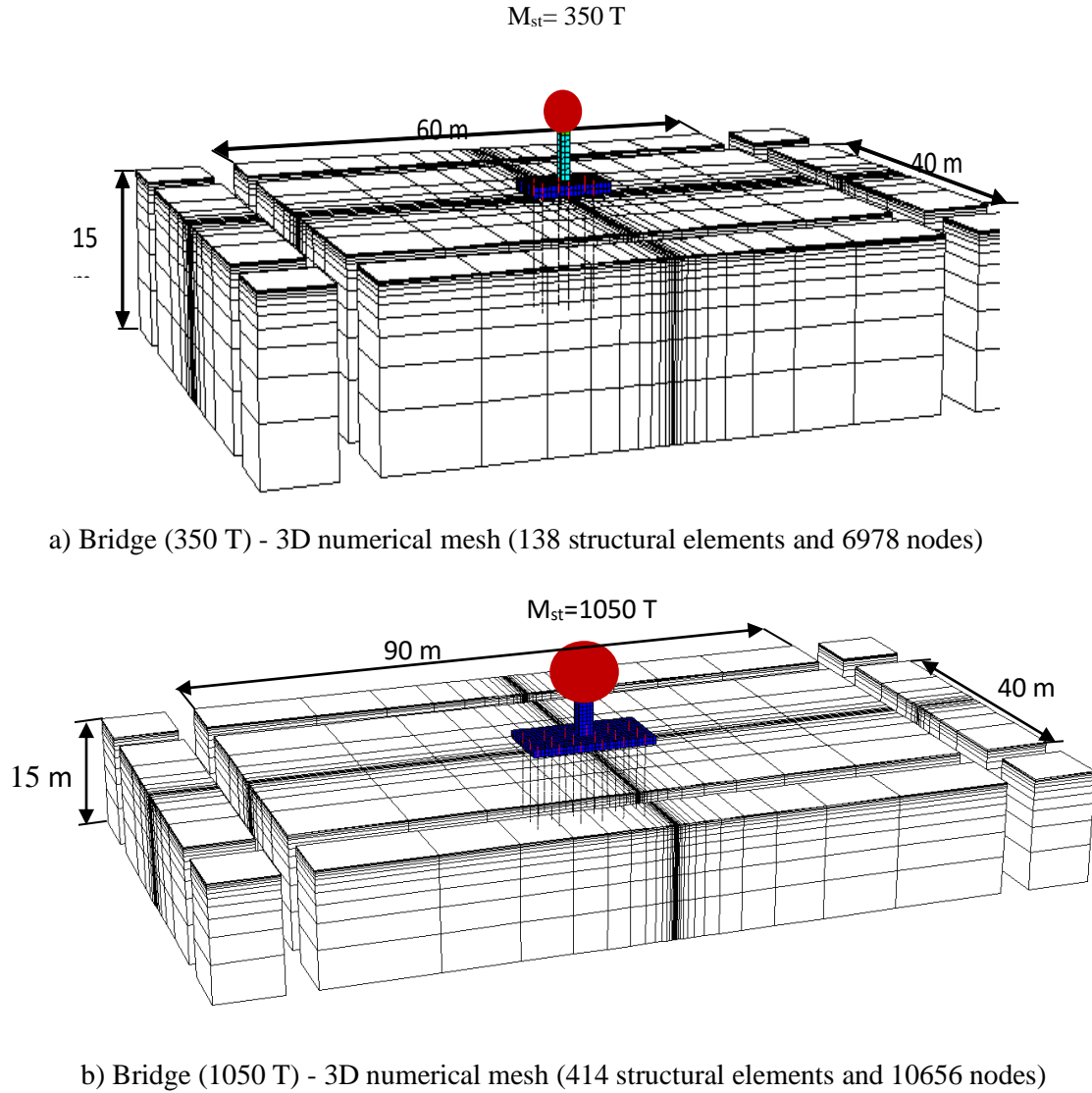
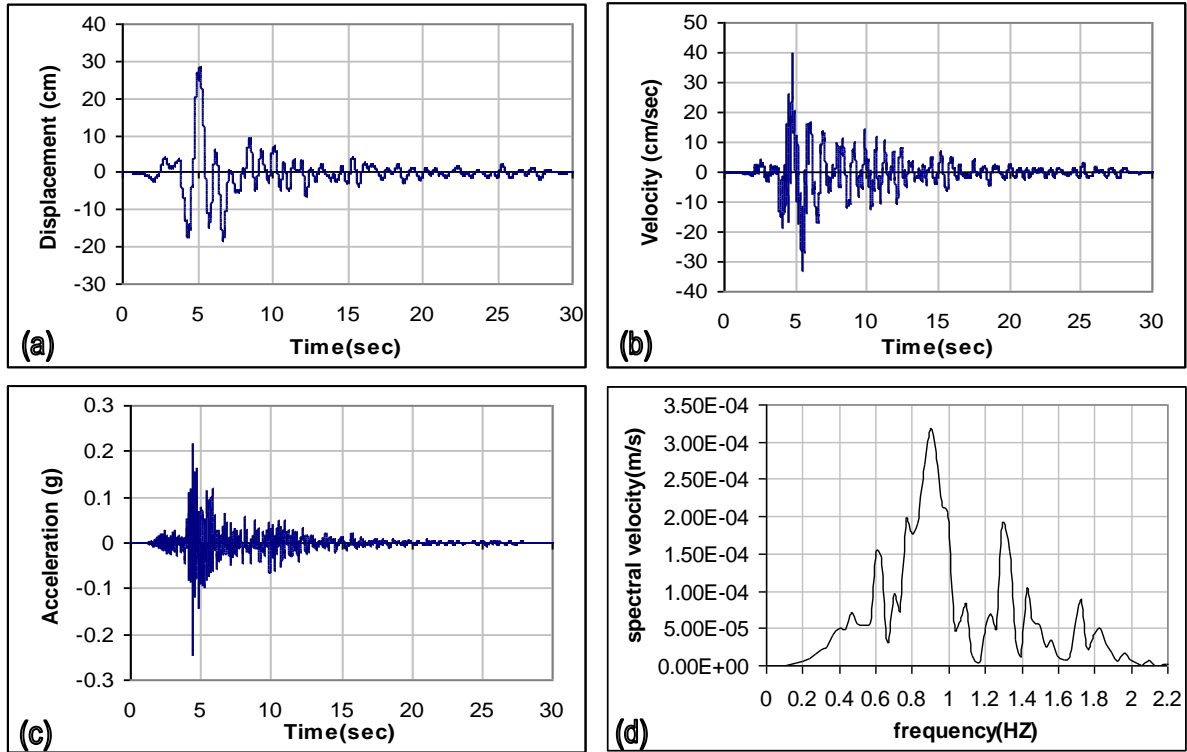


**Fig. 2** 3D numerical mesh of Soil-Piles-Bridge System.

## 2.2 Seismic excitation

The Kocaeli Earthquake ( $M_w = 7.4$ ) occurred on August 17, 1999, in northwestern Turkey (Station AMBARLI; KOERI source) were applied as seismic loading in form of speed at the base of the soil as shown in figure (2). The duration of this seismic record ( $t = 30.08 \text{ sec}$ ) and the peak ground velocity and acceleration of this earthquake are ( $PVA = 40 \text{ cm/s}$ ) and ( $PGA = 0.247 \text{ g}$ ) respectively. As the seismic numerical analyses of (SSSI) is very costly in terms of time and computing power, hence, all the numerical analyses in this study have been implemented for the duration of ( $t = 8.465 \text{ sec}$ ) after a rigorous inspection process to secure that the impacts of this seismic excitation for the duration ( $t = 8.465 \text{ sec}$ ) perfectly equalize the impacts of the whole seismic record duration ( $t = 30.08 \text{ sec}$ ). The Fourier spectrum of the used seismic excitation

shown in figure (3) illustrated the maximum peak is ( $F= 0.9$  Hz) which is between the flexible frequency of the structure ( $F_{ss} = 0.7$  Hz) fundamental frequency of the soil ( $F_1 = 3.2$  Hz), for this reason, this seismic loading has been used in these analyses.



a) Displacement, b) Velocity, c) Acceleration, d) Fourier Spectra of Velocity Component.

**Fig. 3** Kocaeli earthquake record (1999)

### 2.3 Results and Discussion

Results for the bridge of ( $M_{st}= 350$  T) presented in table 4 and figures (4) and (5) reveal significant internal forces in the upper and central parts of the piles, accompanied by a considerable amplification factor at the mass ( $A_{amp} = 10.8$ ).

**Table 4.** response of a group of (2\*3) piles for Kocaeli earthquake (1999).

C Cohesion (KPa)	$a_{st}$ (m/s <sup>2</sup> )	$a_{Cap}$ (m/s <sup>2</sup> )	Internal forces			
			Central piles		Corner Piles	
			$M_{max}$ Bending Moment (KN.m)	$T_{max}$ Shear Force (KN)	$M_{max}$ Bending Moment (KN.m)	$T_{max}$ Shear Force (KN)
150	23.02	14.39	2244	1218	2189	1604

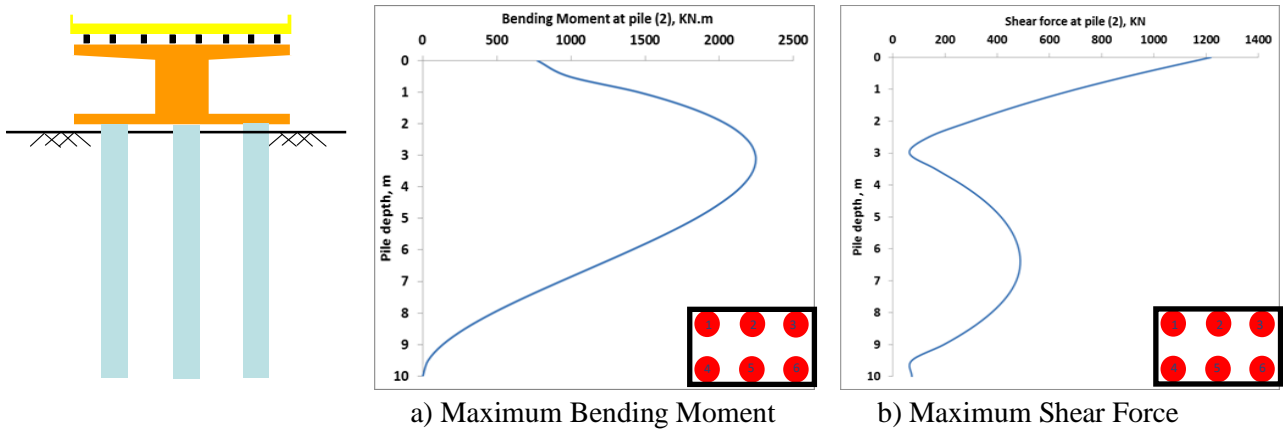


**Fig. 4** Internal forces at central pile (2).

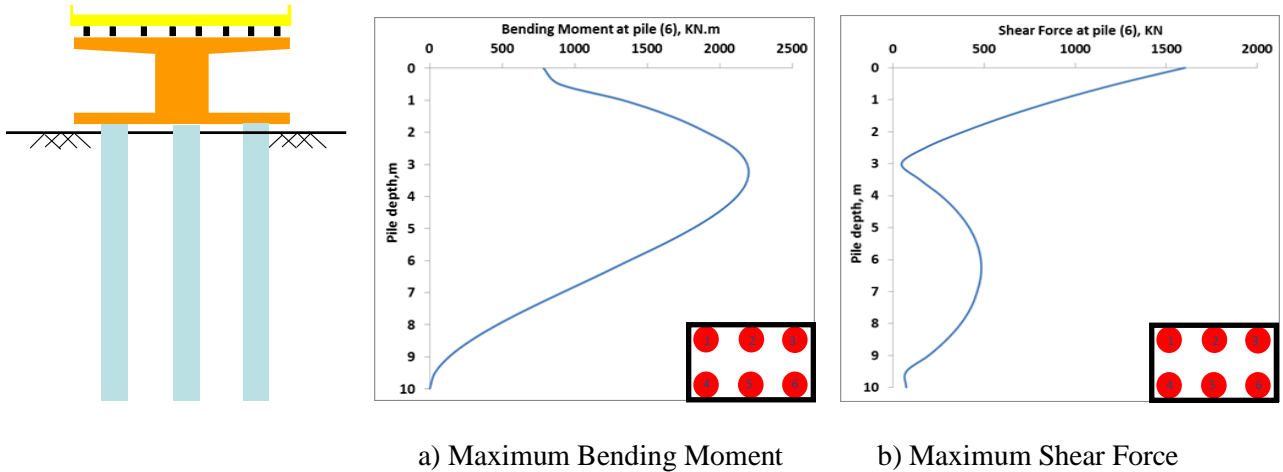


**Fig. 5** Internal forces at corner pile (6).

As seen from table 5 the acceleration of the mass and that cap for the bridge of mass ( $M_{st} = 1050$  T) decreased sensibly, as well as the amplification factor of the Mass ( $A_{amp} = 5.64$ ). Furthermore, the internal forces presented in the figures (6) and (7) shows the maximum bending moment ( $M = 2947$  KN.m) accompanied by the minimum shear force ( $T = 623.3$  KN) for the superstructure masses ( $M_{st} = 350$ , and  $1050$  T).



**Table 5.** response of a group of (6\*3) piles for Kocaeli earthquake (1999).

C (kPa)	$a_{st}$ (m/s <sup>2</sup> )	$a_{Cap}$ (m/s <sup>2</sup> )	Internal forces			
			Central piles		Corner Piles	
			$M_{max}$ (kN.m)	$T_{max}$ (kN)	$M_{max}$ (kN.m)	$T_{max}$ (kN)
150	11.99	10.82	2363	623.3	2947	1007

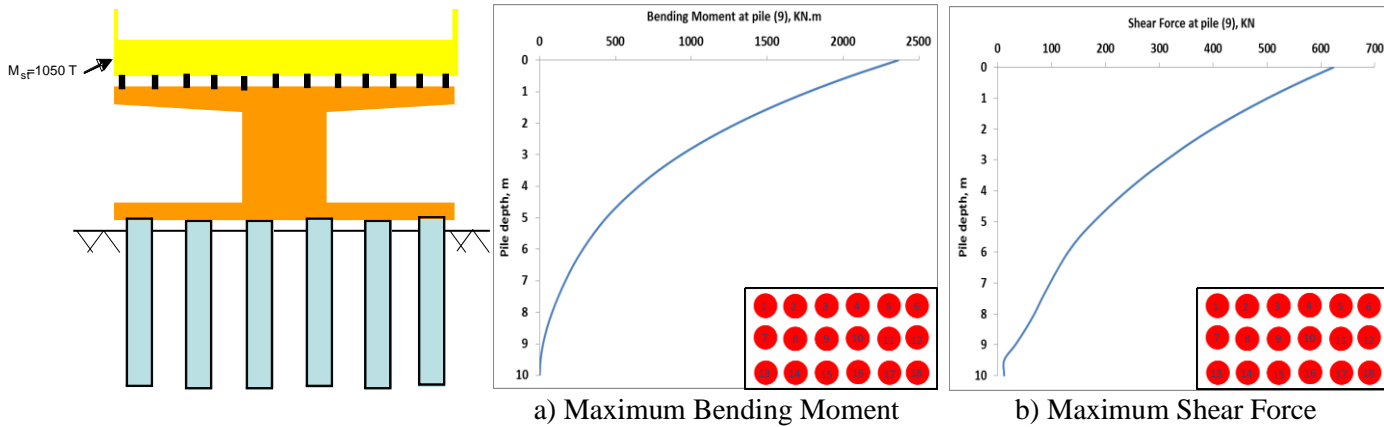


**Fig. 6** Internal forces at central pile (9).

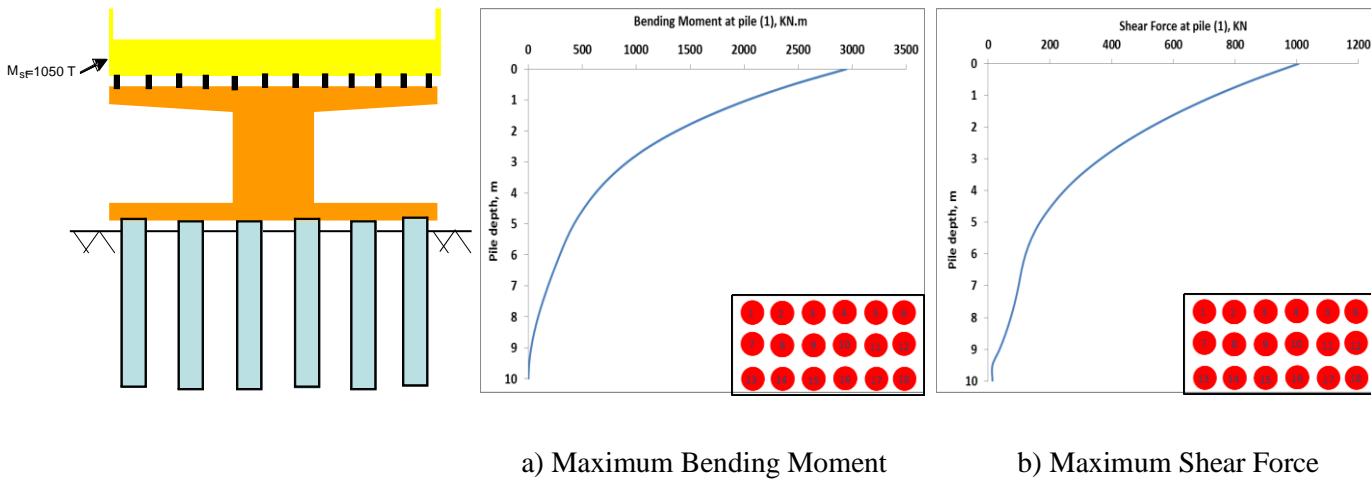


**Fig. 7** Internal forces at corner pile (1).

### 3 Bridge-Soil-Bridge System

The following numerical simulations have been carried out for several configurations of three dissimilar bridges for two superstructure mass ratios (300 %). The impact superstructure height ratios (R) (R=1,1.1,1.15, 1.2, 1.25, 1.5, 2, and 3) for inter-bridge spacing (S=20 m) has been investigated.

### 3.1 Three bridges with superstructure mass ratio (300 %)

#### 3.1.1 Effect of superstructure height ratios

The effect of superstructure height ratios on the (SSSI) effect between three different parallel bridges has been numerically analyzed; the central bridge is the heavier one with a superstructure mass of ( $M_{st}=1050$  T) (figure 2.b) located between two lighter bridges with a superstructure mass of ( $M_{st}=350$  T) (figure 2.a). The numerical calculations were undertaken for a range of height ratios ( $R$ ), precisely ( $R=1, 1.1, 1.15, 1.2, 1.25, 1.5, 2, \text{ and } 3$ ). All the geometrical and mechanical characteristics of soil and concrete mentioned in section (2.1) and tables (1, 2, and 3) have been adopted in these analyses. The numerical simulation is performed for the seismic loading of the Turkey earthquake (Kocaeli,1999). The applied mesh presented in figure (8) includes (4176) zones of 8 node solid elements and (552) three-dimensional structural elements of 2 node beam elements.

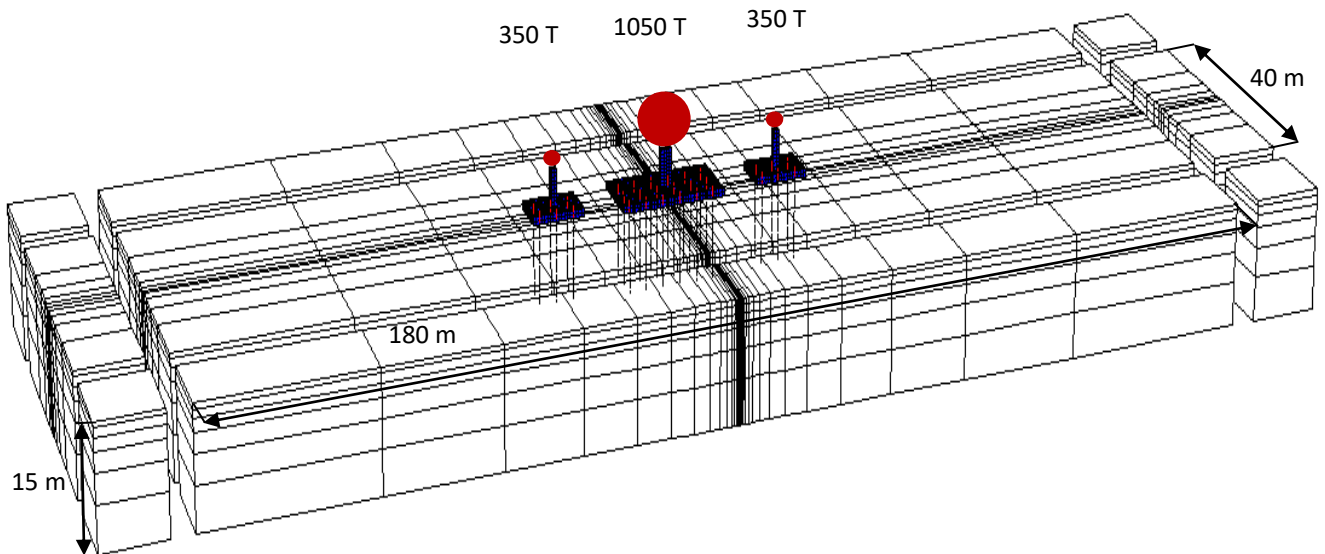
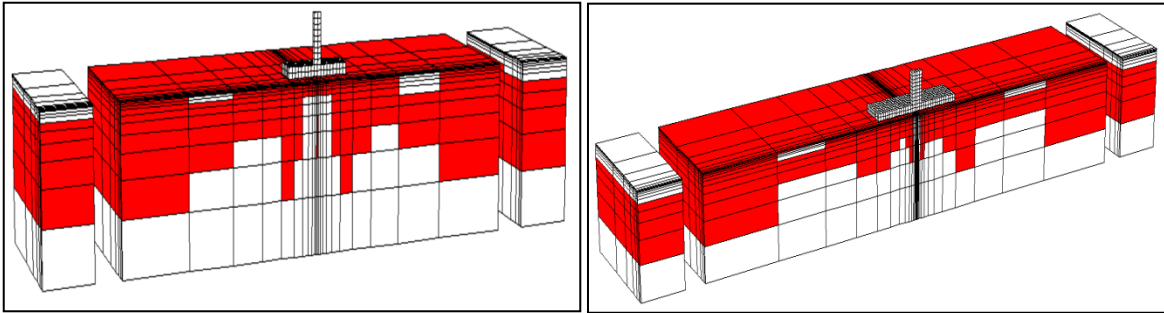


**Fig. 8** Parallel bridges System 3D numerical mesh with adsorbing boundaries

(552 structural elements and 33072 nodes)

#### 3.1.1.1 Results and Discussion

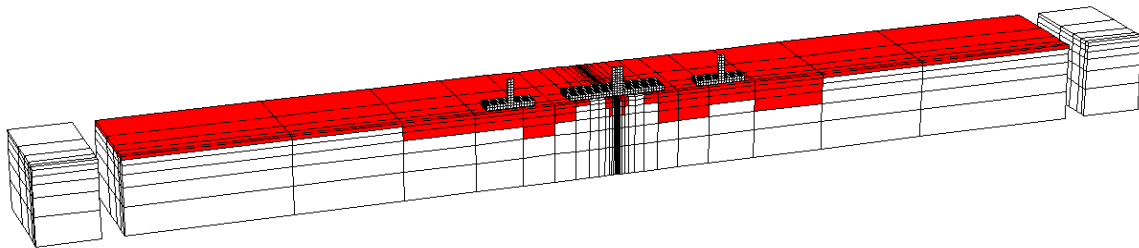
Figure (9) shows that the soil plasticity extension under one isolated single bridge of ( $M_{st}=1050$  T) is denser than that under the bridge of ( $M_{st}=350$  T) wherein the plasticity has prolonged deeper under the cap edges in the x-direction. Interestingly, the plasticity extension under the composition of three parallel dissimilar bridges changed slightly with the variation of the height ratios ( $R=1, 1.1, 1.15, 1.2, 1.25, 1.5, 2$ ). Conversely, the plasticity in the soil has decreased hugely for height ratio of ( $R=3$ ).



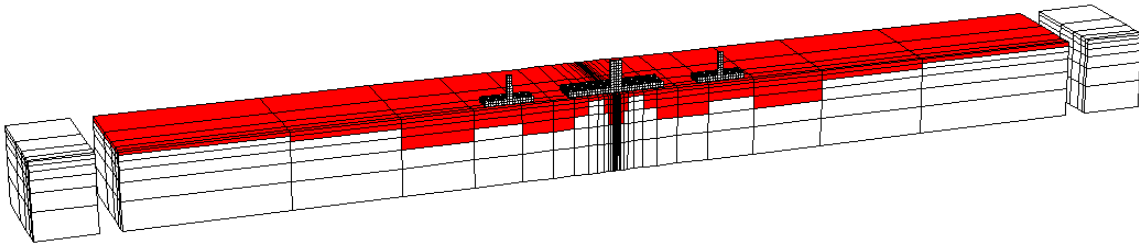
a) One bridge ( $M_{st}=350$  T)

b) One bridge ( $M_{st}=1050$  T)

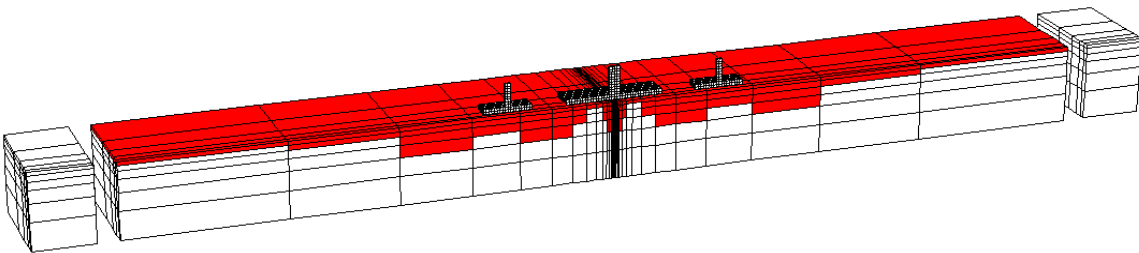
**Fig. 9** Distribution of plasticity (red zones) for two single isolated bridges ( $M_{st}=350$  T) and ( $M_{st}=1050$  T).



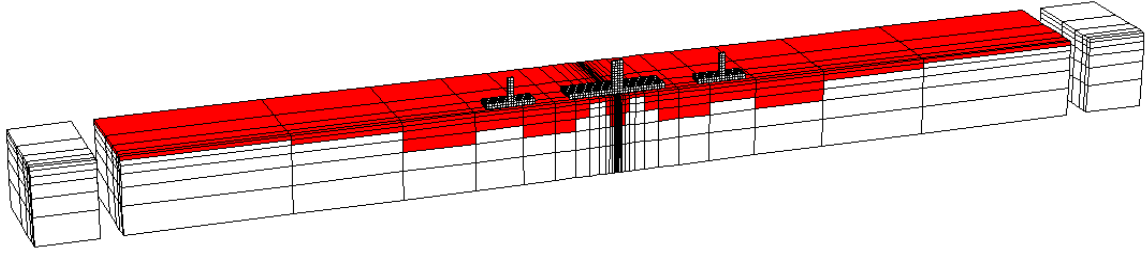
a) Three bridges ( $R=1$ )



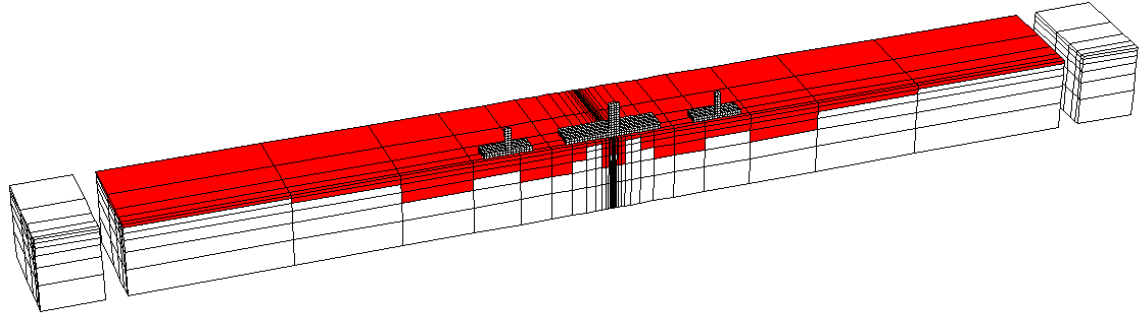
b) Three bridges ( $R=1.1$ )



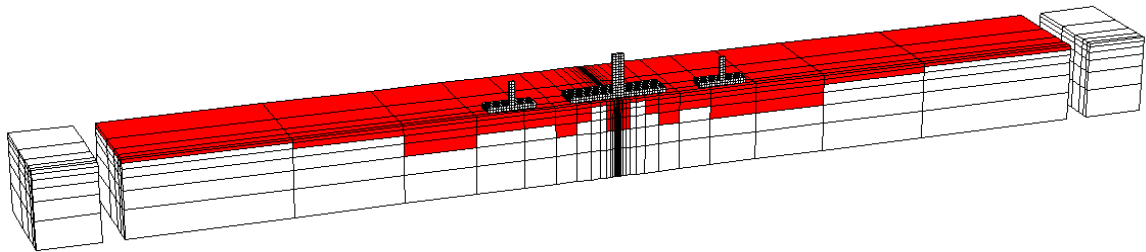
c) Three bridges ( $R=1.15$ )



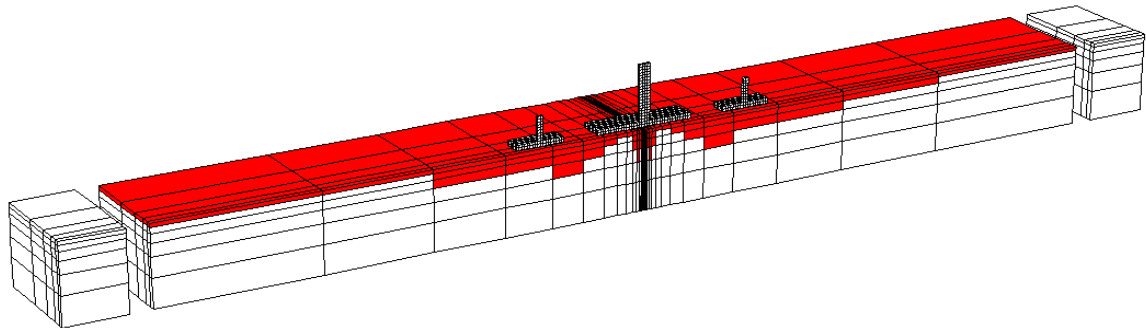
d) Three bridges (R=1.2)



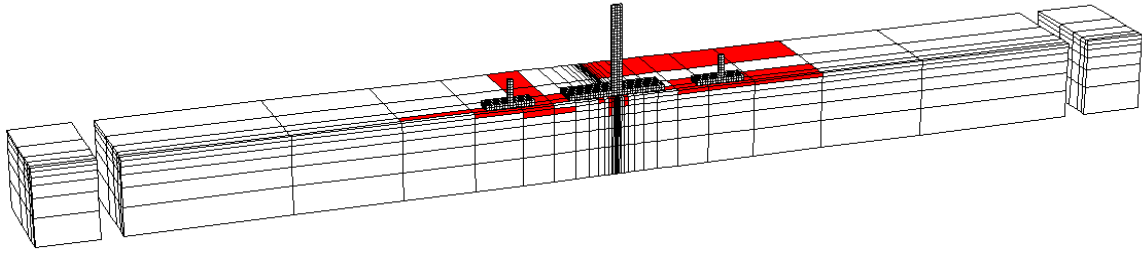
e) Three bridges (R=1.25)



f) Three bridges (R=1.5)



g) Three bridges (R=2)



h) Three bridges (R=3)

**Fig. 10** Distribution of plasticity (red zones) for different height ratios between the three dissimilar bridges ( $M_{st}= 350 T$ ,  $M_{st}= 1050 T$ ,  $M_{st}= 350 T$ )

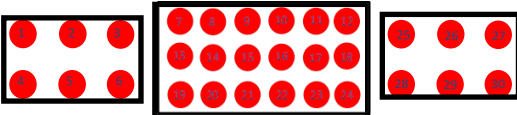


**Table 6** Influence of the height ratio on the seismic response of three dissimilar bridges system

Height Ratio (R)	$a_{st}$ (m/s <sup>2</sup> )		$a_{Cap}$ (m/s <sup>2</sup> )		Internal forces							
					Central piles				Corner Piles			
					Pile (2) ( $M_{st}=350$ T)		Pile (15) ( $M_{st}=1050$ T)		Pile (1) ( $M_{st}=350$ T)		Pile (7) ( $M_{st}=1050$ T)	
					$M_{max}$ (kN.m)	$T_{max}$ (kN)	$M_{max}$ (kN.m)	$T_{max}$ (kN)	$M_{max}$ (kN.m)	$T_{max}$ (kN)	$M_{max}$ (kN.m)	$T_{max}$ (kN)
One Bridge $M_{st}=350$ T	23.02		14.39		2244	1218			2189	1604		
One Bridge $M_{st}=1050$ T	18.09		14.9				2196	1325			1732	1233
Height Ratio (R)	Bridge ( $M_{st}=350$ T)		Bridge ( $M_{st}=1050$ T)		Three dissimilar bridges							
	$a_{st}$	$a_{cap}$	$a_{st}$	$a_{cap}$	Pile (2) ( $M_{st}=350$ T)		Pile (15) ( $M_{st}=1050$ T)		Pile (1) ( $M_{st}=350$ T)		Pile (7) ( $M_{st}=1050$ T)	
1	11.7	11.6	5.79	4.58	2091	1189	1260	294.8	1929	1236	1496	426.3
1.1	11.8	6.4	9.3	5.5	2194	1224	1790	776.4	2026	1326	2395	943.5
1.15	11.5	6.3	9.6	5.7	2142	1203	1725	610.5	1978	1302	2367	957.7
1.2	11.3	6.3	9.7	5.5	2077	1178	1654	616.7	1917	1271	2330	964.5
1.25	11	6.2	9.9	5.3	1998	1147	1568	617.5	1843	1231	2277	964.6
1.5	9.6	5.8	9.2	4.5	1617	988.1	1143	556.5	1486	999.9	1931	906.2
2	9.8	5.5	6	2.1	1719	998.7	899.6	293.9	1566	1036	1184	592.8
3	2.3	1.1	1.1	1.9	630	212.3	641.1	91.73	542.6	241.1	844.8	153.1

Table. 6 demonstrates the vital positive effect of the (SSSI) on both of the superstructure acceleration and by smaller ratio on the internal forces induced in the piles. The mass acceleration of the light bridge of ( $M_{st} = 350$  T) declines considerably (49.17 %) as a result of the (SSSI) effect; likewise, the mass acceleration of the heavy bridge of ( $M_{st} = 1050$  T) decreases hugely by (68%). Identically, the cap acceleration of the heavy bridge of ( $M_{st} = 1050$  T) and the light bridge ( $M_{st} = 350$  T) falls by (up to 69.26 %, and 19.38 %) respectively. Concerning the effect of (SSSI) on the internal forces induced in the piles, the bending moment and the shear force induced in the piles of the heavy bridge of ( $M_{st} = 1050$  T) reduced by (up to 42.6 % and 77.75 %) respectively as illustrated in table (7) . Alike, table (7) exhibits a close impact of the (SSSI) on the piles of the light bridge of ( $M_{st} = 350$  T) via decreasing the bending moment and the shear force by (up to 11.87 % and 22.94 %) respectively. In consequence, the interaction between three dissimilar bridges (SSSI) has effective beneficial impacts on the superstructure acceleration and the piles internal forces by inducing a substantial decline of both. Table 6 and Figures 11, and 12 demonstrate the essential influence of the increasing of height ratio by (10 %) for height ratio of ( $R= 1.1$ ) on the internal forces provoked in the piles of the heavy bridge of ( $M_{st} = 1050$  T) through considerable rise in bending moment (up to 60 %) and huge augment of shear force by (up to 263.36 %). Whereas, the bending moment and shear force induced in the piles of the light bridge of ( $M_{st} = 350$  T) have slightly decreased by (5 % and 7.28 %) respectively for height ratio of ( $R=1.1$ ) as shown in table 6 and figures 13, and 14. Generally, the rise of height ratios in the range of ( $R= 1.15, 1.2, 1.25, 1.5, 2$ ) caused a sensible reduction of the bending moment by (up to 38.7 %) and the shear force by (up to 47.18 %) induced in the piles of the heavy bridge of ( $M_{st} = 1050$  T). Similarly, the bending moment and the shear force induced in the piles of the light bridge of ( $M_{st} = 350$  T) have dropped with the increase of the height ratios in the range of ( $R= 1.15, 1.2, 1.25, 1.5, 2$ ) by (up to 19 %) and (18.77 %) respectively. It is worth mentioning that all the minimum internal forces induced in the piles of both heave ( $M_{st} = 1050$  T) and light bridge ( $M_{st} = 350$  T) have been obtained for height ratio ( $R= 3$ ) through immense decline in bending moment (up to 65.35 %) and in shear force (up to 78.7 %).

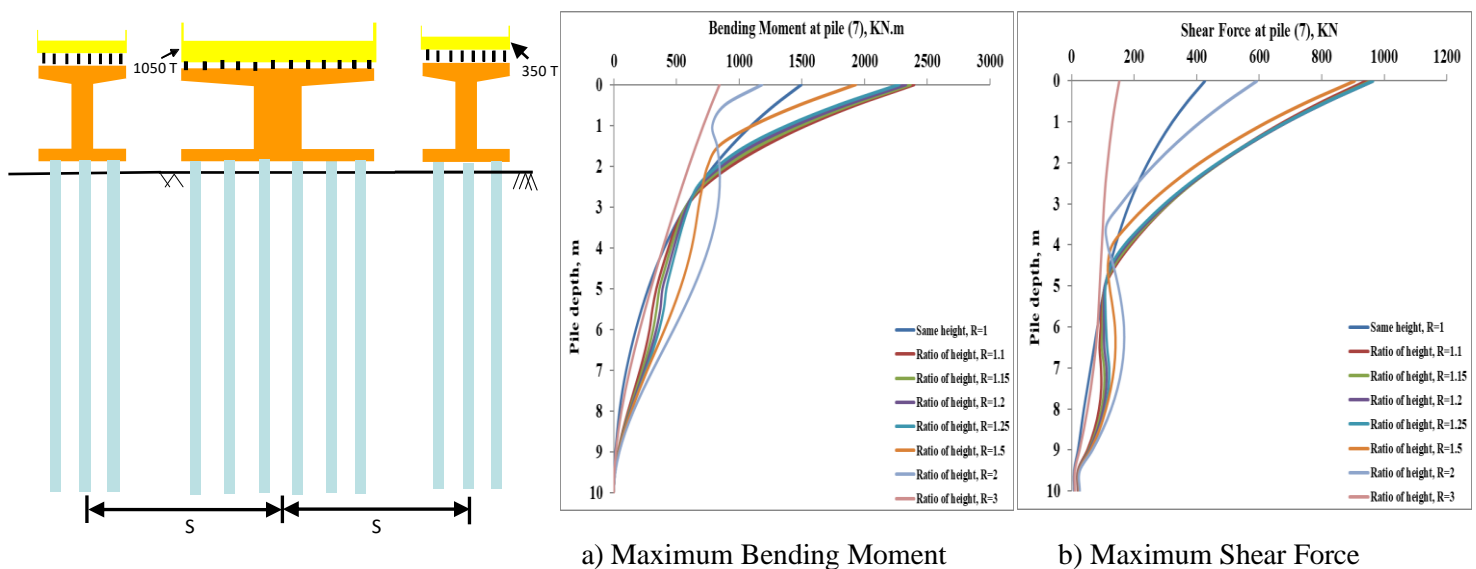
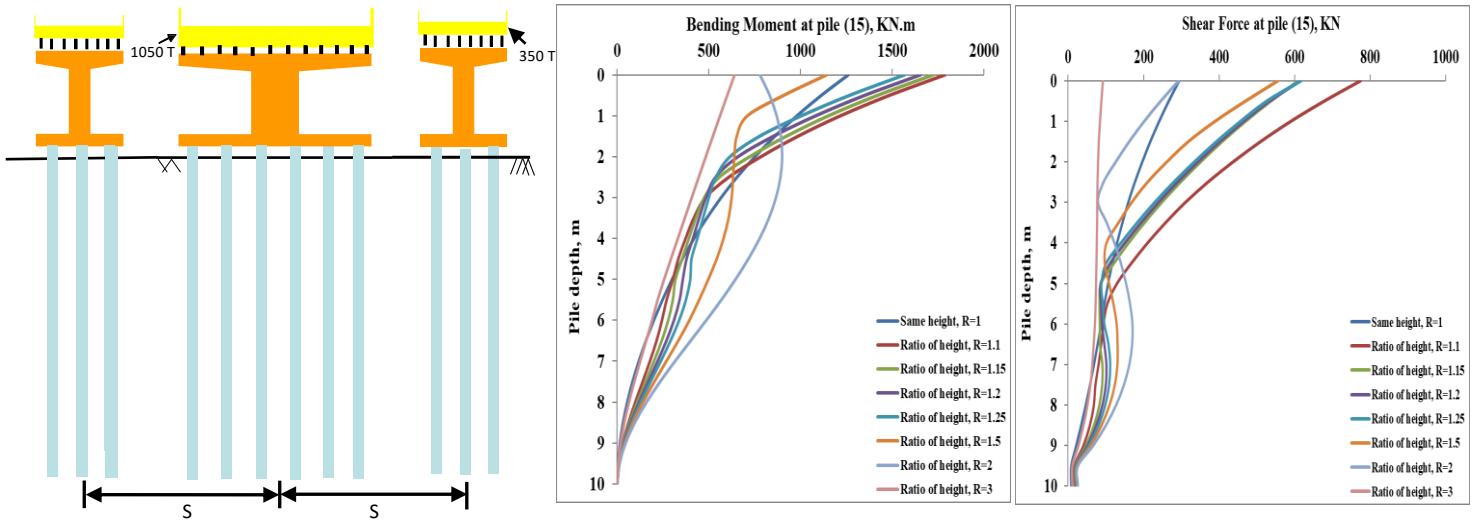
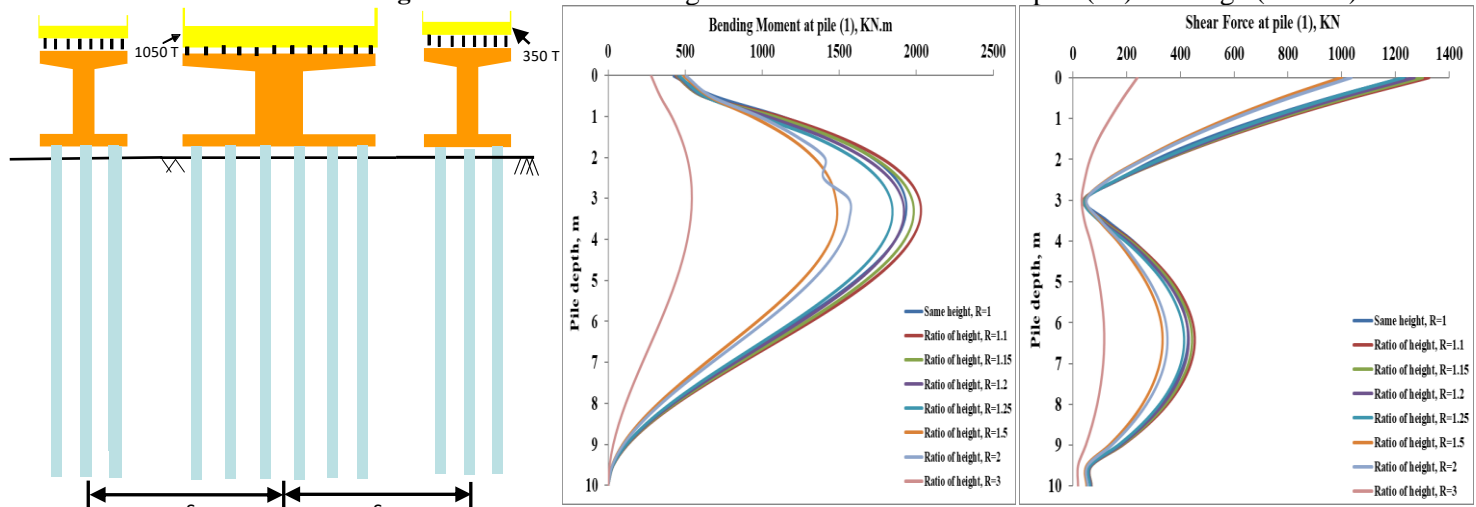


**Fig. 11** Three dissimilar bridges: Internal forces at corner pile (7) of bridge (1050 T)



a) Maximum Bending Moment      b) Maximum Shear Force

**Fig. 12** Three dissimilar bridges: Internal forces at central pile (15) of bridge (1050 T)

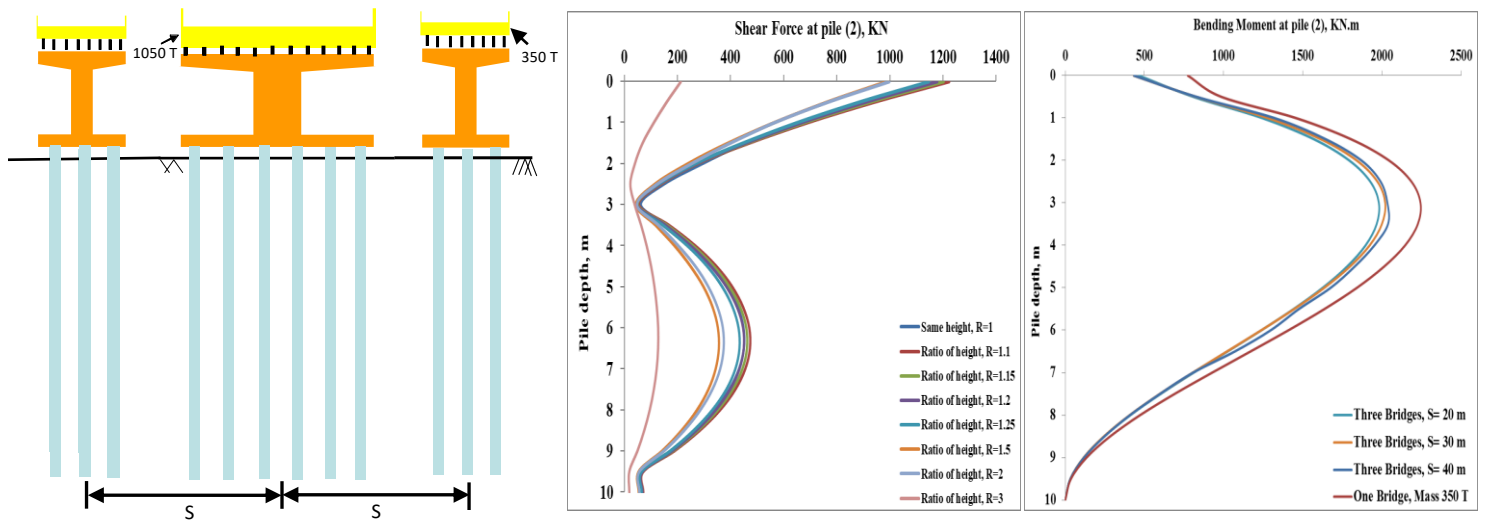


a) Maximum Bending Moment      b) Maximum Shear Force

**Fig. 13** Three dissimilar bridges: Internal forces at corner pile (1) of bridge (350 T)

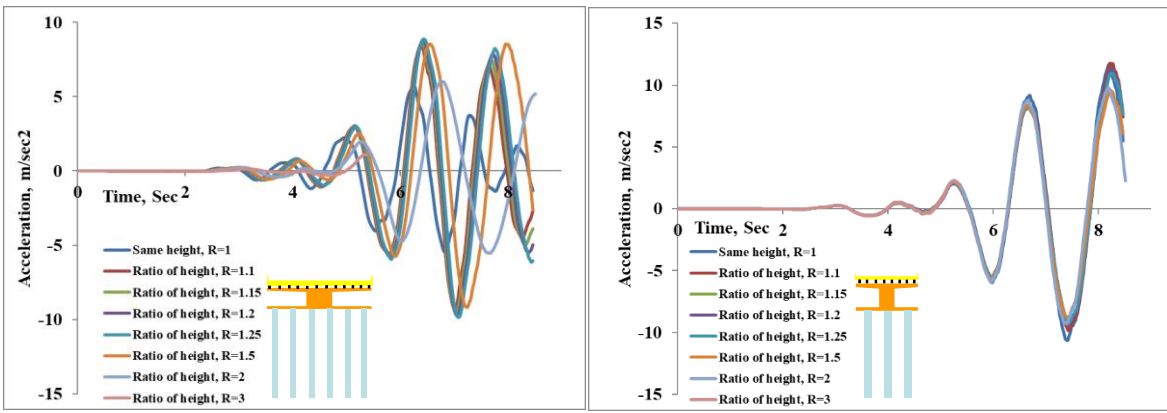
In terms of the superstructure's masses accelerations, the mass acceleration of the heavy bridge of ( $M_{st} = 1050 T$ ) increased maximumly by (70.9 %) with the rise of the height ratios in the range of ( $R=1.1, 1.15, 1.2, \text{ and } 1.25$ ), then the acceleration reduced immensely by (81%) for height ratio of ( $R=3$ ) as presented in figure(15a). While, the mass acceleration of the light bridge of ( $M_{st} = 350 T$ ) decreased fairly by (16.23 %) with the rise of the height ratios in the range of ( $R=1.1, 1.15, 1.2, 1.25, 1.5, \text{ and } 2$ ) and hugely by (80.34 %) for height ratio of ( $R=3$ ) as shown in figure (15b).





a) Maximum Bending Moment      b) Maximum Shear Force

**Fig. 14** Three dissimilar bridges: Internal forces at central pile (16) of bridge (350 T)



a) Mass (1050 T) Acceleration      b) Mass (350 T) Acceleration

**Fig. 15** Three dissimilar bridges: Masses Accelerations.

Figure (16) displays the velocity spectral analysis of Fourier for both the lateral seismic responses of the superstructure mass of ( $M_{st} = 1050 \text{ T}$ ) and the superstructure mass of ( $M_{st} = 350 \text{ T}$ ) under the loading of Turkey (1999) for the studied height ratios ( $R= 1, 1.1, 1.15, 1.2, 1.25, 1.5, 2,$  and  $3$ ). The dominant frequency of the superstructure mass of ( $M_{st} = 1050 \text{ T}$ ) has dropped from ( $F= 0.709 \text{ Hz}$ ) for the height ratios in the range of ( $R=1, 1.1, 1.15, 1.25,$  and  $1.5$ ) to ( $F= 0.373 \text{ Hz}$ ) for height ratio of ( $R= 3$ ). In contrast, the dominant frequency for the bridge of ( $M_{st} = 350 \text{ T}$ ) stills constant ( $F= 0.591 \text{ Hz}$ ) for all the height ratios ( $R= 1, 1.1, 1.15, 1.2, 1.25, 1.5,$  and  $3$ ) except for the height ratio of ( $R= 2$ ) where the dominant frequency is ( $F= 0.236 \text{ Hz}$ ).

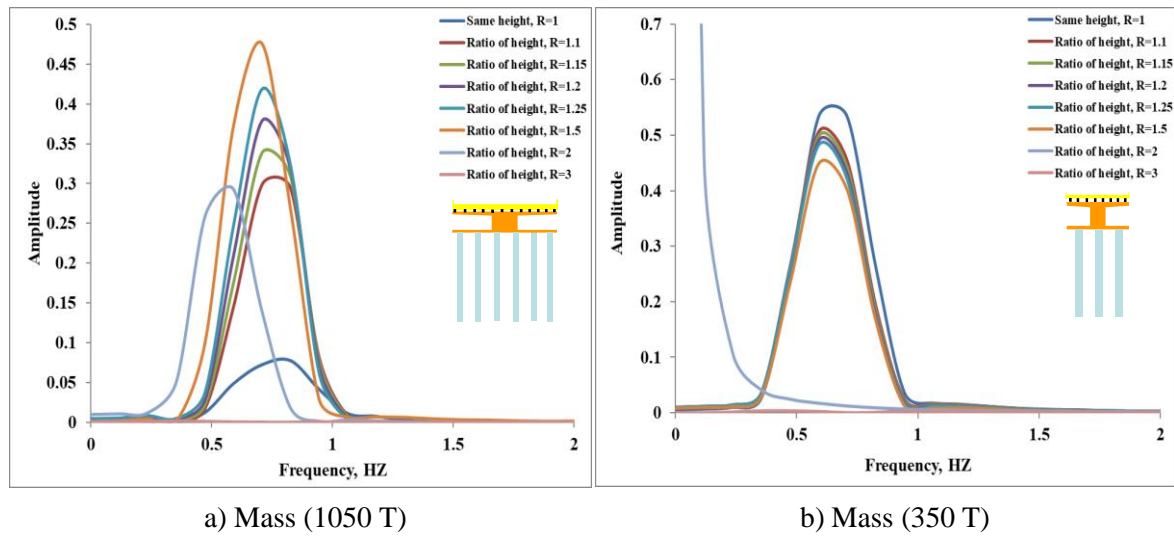


**Fig. 16** Three dissimilar bridges: Fourier spectra diagram.

#### 4 Conclusions

This paper presents a thorough detailed dynamic analyses of seismic bridge-soil-bridge interaction to explore the mechanisms of through-soil interaction between three dissimilar neighboring bridges focusing on the effect of the superstructure height ratios ( $R=1, 1.1, 1.15, 1.2, 1.25, 1.5, 2,$  and  $3$ ). The numerical analyses have been performed by using three-dimensional code (FLAC 3D) based on the finite-difference elements method. The behavior of the concrete structural elements of the superstructure and the foundation was assumed as linear behavior in the 3D numerical simulation, while non-linear elastoplastic behavior has been employed to simulate the real dynamic behavior of the soil in these numerical analyses. The numerical analyses were carried out using the real earthquake record of Turkey (Kocaeli 1999).

The main question of this research is in what situations the superstructure height ratio impact on Seismic Structure-Soil-Structure Interaction (SSSI) could be beneficial or detrimental for the individual elements of the system?

This research has led to the following principal conclusions based on the cases studied:

- Intriguingly, the results revealed substantial beneficial effects for high superstructures height ratios ( $R= 2,$  and  $3$ ) on the bending moment induced in the piles of the heavy bridge of ( $M_{st} = 1050 T$ ) through huge reduction (up to 50 %). Similarly, the shear force dropped massively (up to 68.88 %) for height ratio ( $R= 3$ ). Conversely, the small height ratios ( $R= 1.1, 1.15, 1.2, 1.25,$  and  $1.5$ ) have detrimental on both bending moment and shear force represented by immense increase (up to 60 %) and (up to 226.27 %) respectively.

- Likewise, the high height ratios ( $R=1.25, 1.5, 2$  and  $3$ ) have positive effects on both bending moment and shear force induced in the piles of the light bridge of ( $M_{st} = 350 T$ ) through reduction (up to 71.87 % and 82.14 %) respectively. While, the small height ratios ( $R= 1.1, 1.15,$  and  $1.2$ ),

generally have rather a neutral impact on both bending moment and shear force incited in the piles.

- Overall, the rise of the height ratios has important positive impact on both the mass acceleration of the light bridge of ( $M_{st} = 350$  T) and the heavy bridge of ( $M_{st} = 1050$  T) with huge decrease ratios (80.34 %) and (81%) respectively.

## References

[1] Ada, M., and Ayvaz, Y., 2019. The structure-soil-structure interaction effects on the response of the neighbouring frame structures. *Latin American Journal of Solids and Structures*, 16(8), e224. <https://doi.org/10.1590/1679-78255762>

[2] Alam, Md Iftekharul., Kim, Dookie., 2014. Spatially varying Ground Motion Effects on Seismic Response of Adjacent Structures Considering Soil-Structure Interaction. *Advances in Structural Engineering*, Vol. 17 No. 1 2014. <https://doi.org/10.1260/1369-4332.17.1.131>

[3] Alfach, Mohanad Talal., 2021. Seismic structure-soil-structure interaction between two different adjacent piled bridges founded in nonlinear soil. *Geomechanics and Geoengineering*. <https://doi.org/10.1080/17486025.2021.1928764>

[4] Alexander, Nicholas A., Ibraim, E and Aldaikh, H., 2013. A simple discrete model for interaction of adjacent buildings during earthquakes. *Computers & Structures*, Vol. 124, 1-10. <https://doi.org/10.1016/j.compstruc.2012.11.012>

[5] Chopra, A. K., 2012. Dynamics of structures theory and applications to earthquake engineering (4th ed., p. 757). Upper Saddle River: Prentice Hall. *Chopra, Dynamics of Structures, Global Edition, 4th Edition | Pearson*

[6] Bolisetti, C., and Whittaker, A.S., 2020. Numerical investigations of structure-soil-structure interaction in buildings, *Engineering Structures*, 215 – 110709. <https://doi.org/10.1016/j.engstruct.2020.110709>

[7] Bybordiani, M., and Arici, Y., 2019. Structure-soil-structure interaction of adjacent buildings subjected to seismic loading. *Earthq. Eng. Struct. Dyn.*, 48, 731–748. <https://doi.org/10.1002/eqe.3162>

[8] Gan, Jinsong., Li, Peizhen and Liu, Qiang., 2020. Study on dynamic structure-soil-structure interaction of three adjacent tall buildings subjected to seismic loading. *Sustainability*, 12(1), 336. <https://doi.org/10.3390/su12010336>

[9] Ghandil, M., & Aldaikh, H., 2016. Damage-based seismic planar pounding analysis of adjacent symmetric buildings considering inelastic structure-soil-structure interaction. *Earthquake Engineering & Structural Dynamics*, Vol.46, Issue7. <https://doi.org/10.1002/eqe.2848>

[10] Ghiocel, D.M., Bogdan, O., & Cretu, D., 2014. Seismic structure soil-structure interaction (SSSI) effects for dense urban areas. *Second European conference on earthquake engineering and seismology*, Istanbul Aug. 25-29.

- [11] Liang, J.W., Han, B., Todorovska, M.I., Trifunac, M.D., 2018. 2D dynamic structure-soil-structure interaction for twin buildings in layered half-space II: Incident SV-waves. *Soil Dyn. Earthq. Eng.*, 113, 356–390. <https://doi.org/10.1016/j.soildyn.2018.05.023>
- [12] Rahgozar, M.A., 2015. Accounting for soil nonlinearity in three-dimensional seismic structure-soil-structure-interaction analyses of adjacent tall buildings structures. *International journal of civil engineering*, 13 (3 and 4B) ,213-225. DOI: 10.22068/IJCE.13.3.213
- [13] Vicencio, F., Alexander, N.A., 2018. Higher mode seismic structure-soil-structure interaction between adjacent building during earthquakes. *Eng. Struct.*, 174, 322–337. <https://doi.org/10.1016/j.engstruct.2018.07.049>
- [14] Vicencio, Felipe., Alexander, Nicholas A., 2019. Dynamic Structure-Soil-Structure Interaction in unsymmetrical plan buildings due to seismic excitation. *Soil Dyn. Earthq. Eng.*, 127, 105817. <https://doi.org/10.1016/j.soildyn.2019.105817>
- [15] Wang, Huai-feng., 2018. Structure-soil-structure interaction between underground structure and surface structure, Earthquakes - Forecast, *Prognosis and Earthquake Resistant Construction*, Valentina Svalova, IntechOpen. DOI: 10.5772/intechopen.76243